

DETERMINATION OF ILLITE-SMECTITE STRUCTURES USING MULTISPECIMEN X-RAY DIFFRACTION PROFILE FITTING

BORIS A. SAKHAROV, HOLGER LINDGREEN,¹ ALFRED SALYN, AND VICTOR A. DRITS

Institute of Geology, Russian Academy of Sciences, Pyzhevsky per D.7., 109017 Moscow, Russia

¹ Clay Mineralogical Laboratory, Geological Survey of Denmark and Greenland, Thoravej 8, DK2400 Copenhagen NV, Denmark

Abstract—A procedure for structural investigations by X-ray diffraction of mixed-layer structures incorporating swelling layers has been developed. For each sample, specimens saturated with different cations (Na, Mg, and Ca), are analyzed both as air-dried and as glycolated. One structural model fitting all the observed patterns then provides the structure of the sample. Samples tested include: Illite-smectite (I-S) minerals from Kazakhstan (a rectorite), Dolna Ves in Slovakia, Kinnekulle in Sweden, the North Sea, and Scania in Sweden. The fitting of the patterns of the Kazakhstan rectorite demonstrated that the instrumental parameters applied in the modeling were correct. For the I-S minerals from Slovakia and Kinnekulle the observed patterns were fitted with one two-component I-S model. However, the Ca-saturated and air-dried specimen of the Kinnekulle bentonites had two types of swelling interlayers. For the Slovakian I-S with Reichweite = 2, an alternative two-phase I-S plus I-V (V = vermiculite) model fitted the experimental X-ray diffraction patterns equally well. The I-S mineral from Scania is in fact a three-component I-T-S (T = tobelite) and the North Sea sample is a four-component I-S-V-V', one type of the swelling layers having swelling characteristics intermediately between smectite and vermiculite. In addition to layer types and distribution, interlayer compositions, such as the amount of interlayer glycol and water and of fixed and exchangeable cations, were determined.

Key Words—Illite-Smectite, Simulation, Structure, Swelling, X-Ray Diffraction.

INTRODUCTION

Determination of the structure of mixed-layer minerals containing illite and swelling layers is important because these are common minerals and diagenesis and weathering changes their structure (Shutov *et al.*, 1969a, 1969b; Perry and Hower, 1970; Weaver and Beck, 1971; Hower *et al.*, 1976). By X-ray diffraction (XRD), the interstratification of illite-smectite (I-S) minerals is usually estimated from peak-migration curves showing the position of basal reflections versus the proportion and mode of interstratification of layer types in the mixed-layer structure (Drits and Sakharov, 1976; Środoń, 1980, 1981, 1984; Watanabe, 1981, 1988; Reynolds, 1980, 1988; Tomita *et al.*, 1988; Moore and Reynolds, 1989; Drits *et al.*, 1994). The peak-migration technique can, however, only be used for two-component I-S with random ($R = 0$, where R is the Reichweite parameter) or maximum ordering for $R = 1, 2$, or 3 , but not for I-S with segregated I or S layers or with intermediate degrees of ordering. Furthermore, peak-migration curves have so far mainly been used for glycolated I-S and are usually based on the assumption that all smectite interlayers contain two glycol layers and that their swelling properties do not depend on the exchangeable cation. In addition, the mica layers are usually assumed to be K-bearing and the thickness to be 9.98 or 10 Å.

The most effective technique for determination of the structural parameters of mixed-layer minerals is based on comparison between experimental XRD

curves and curves calculated for structural models having different proportions and distributions of illite and smectite layers (Reynolds and Hower, 1970; Drits and Sakharov, 1976; Reynolds, 1980; Moore and Reynolds, 1989; Drits and Tchoubar, 1990). However, the simulation of XRD patterns requires many structural and instrumental parameters (*e.g.*, types, structures, compositions, thicknesses, and distribution of layers; mean thickness and thickness distribution of coherent scattering domains (CSD); particle orientation; divergence of initial and diffracted XRD beams) which are known only approximately. For example, the swelling of smectite interlayers depends on the exchangeable cations, the intercalated organic compounds, and the charge of the 2:1 layers, and these parameters require extensive work to determine (Brindley, 1966; MacEwan and Wilson, 1980; Drits *et al.*, 1997a). The effect of these numerous variables is that several structural models may seem to fit the experimental data equally well, especially if the experimental and calculated patterns are not superposed.

The goal of this work is to demonstrate that determination of reliable and detailed structural models for mixed-layer minerals can be obtained by the multispecimen profile fitting procedure: First, for the pattern of each specimen, close agreement between positions, intensities, and profiles of the reflections in the calculated and experimental diffractograms must be obtained. Second, for one and the same sample, calculated XRD patterns for one structural model must fit

the observed patterns of several specimens saturated with different exchangeable cations and examined both as air-dried and as glycolated. The principle of this multispecimen method is that each different treatment of the same sample is an independent test of the statistical structural model because each treatment changes the thickness and scattering efficiency of the swelling layers, but not the 2:1 layers and their distribution. Thus, structural parameters may be determined which are difficult or even impossible to obtain by current techniques. However, the present work demonstrates difficulties in the unambiguous determination of the actual structure of mixed-layer minerals, and I-S in particular.

MATERIALS AND METHODS

Samples

A rectorite-containing sample from the ore mine of Bestude, Kazakhstan (Sakharov and Shlykov, personal communication); a hydrothermal sample DV2 from Slovakia (Šucha *et al.*, 1992); two Kinnekulle bentonites, B32 and B35 (Brusewitz, 1986); an illite-smectite-vermiculite (I-S-V) mixed-layer sample from the Upper Jurassic oil source rock from the Danish onshore well Haldager 1, 1049 m depth (sample 95) and the North Sea well 2/11-1, 4548 m depth (sample 87); and an illite-tobelite-smectite (I-T-S) mixed-layer sample from the Cambrian alum shale from Åkarpssmölle, Scania, Sweden, were investigated.

Sample preparation

The <0.1- μm size fraction of DV2, the <0.2- μm size fraction of the Kinnekulle bentonites, and the rectorite sample were investigated. In shales, discrete illite is often present in addition to mixed-layer I-S (Reynolds and Hower, 1970; Hower *et al.*, 1976; Nadeau and Reynolds, 1981). Thus, illite reflections may mask important features of the illite-smectite XRD pattern. Therefore, a special technique was used to isolate a mixed-layer fraction from the Jurassic and Cambrian shale samples. The samples were gently crushed to pass a 0.125-mm sieve. Chemical pretreatment involved using NaAc at pH 5.5 and 100°C to remove calcite, followed by NaOCl at pH 9.0 and 100°C to remove organic matter (Anderson, 1963), and then Na-dithionite, bicarbonate and citrate at pH 7 to remove Fe- and Al-oxides (Mehra and Jackson, 1958), using ~100 mg of dithionite per g of sample. The sand + silt fraction was then removed by centrifugation and the fine clay (<0.2 μm) and coarse clay (0.2–2 μm) fractions were divided in a continuous-flow centrifuge. Because discrete illite and kaolinite were present in appreciable amounts even in the fine clay fraction of the shale, I-S-V was concentrated in an I-S-V fraction by the ethanol-water procedure of Buzagh and Szepesi (1955). This method was also used by Gibbs (1967)

for the separation of montmorillonite (see Hansen and Lindgreen, 1989). Based on scanning probe microscopy the particles of this fraction are predominantly <500 Å in diameter and <100 Å in thickness (Lindgreen *et al.*, 1992). The fraction is dominated by mixed-layer minerals; other minerals were removed.

Each sample was saturated with K^+ , Na^+ , NH_4^+ , Mg^{2+} , and Ca^{2+} using standard procedures. Oriented mineral aggregate specimens were prepared by the pipette method using 2.5 mg/cm² of specimen. The specimens were then treated with ethylene glycol vapor for 3 d at 60°C.

X-ray diffraction

XRD patterns were obtained using $\text{CuK}\alpha$ and $\text{CoK}\alpha$ radiation with the DRON-4 and Philips PW1050 diffractometers, respectively. The DRON-4 diffractometer was supplied with a graphite monochromator and fine antiscatter slits (0.1–0.25 mm) to limit the horizontal beam divergence, along with soller slits having an angular aperture of 2.5° to limit the vertical beam divergence. Intensities were measured for 100 s per 0.05 °2 θ step. The Philips diffractometer was supplied with Fe-filters and with 1/4° fixed divergence and antiscatter slits. Intensities were measured for 10 s per 0.1°2 θ step. The XRD patterns were fitted within the 2.5–55 °2 θ region using the program of Drits and Sakharov (1976). Corrections for instrumental variables including horizontal and vertical beam divergences, goniometer radius, dimensions and thickness of samples followed the recommendations of Reynolds (1986) and Drits *et al.* (1993).

In the following, I, T, S, and V denotes illite, tobelite, smectite, and vermiculite-like or high-charge smectite layers, respectively, and w_i , w_{ij} , w_{ijk} , *etc.* are the probabilities to find, respectively, a layer *i*, a layer pair *ij*, and a layer triple *ijk*. In addition, p_{ij} denotes the conjunction probability for a layer *j* to follow a layer *i* and p_{ijk} is the conjunction probability for a layer *k* to follow a layer pair *ij* (*i*, *j*, *k* = I, T, S, or V). Note that the use of simulations of XRD patterns permits us to determine the proportions and distribution of interlayers but not the layer types.

Structural models

Models for illite-containing 2:1 mixed-layer structures have 2:1 layers separated by different types of interlayers. For 2:1 layers, *z* coordinates and site occupancies given by Moore and Reynolds (1989, p. 321–322) were used. For most of the studied samples, the structure and composition of air-dried smectite interlayers containing different cations correspond to the one-dimensional structure of Moore and Reynolds (1989, p. 321–322). For the one and two-layer glycol complexes of smectite and vermiculite interlayers, the *z* coordinates and site occupancies of glycol molecules determined by Moore and Reynolds (1989, p. 321–

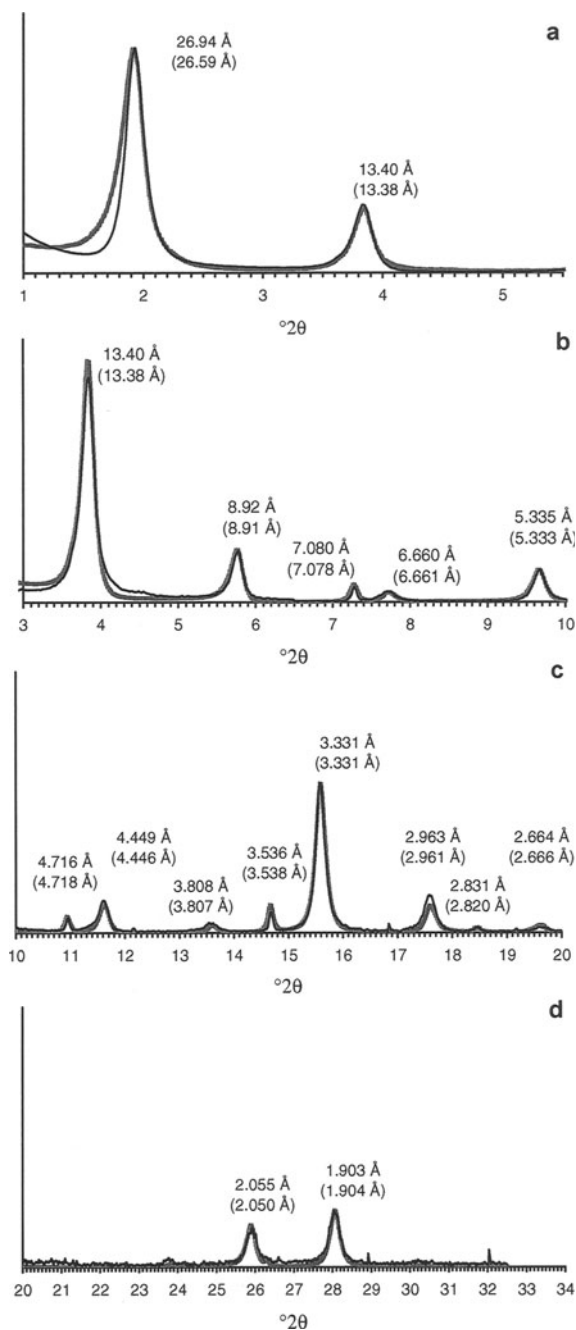


Figure 1. Powder XRD patterns of the rectorite (Kazakhstan) sample. Observed patterns: solid line; simulated: shaded line; d -values for simulated patterns in brackets. Oriented specimen, Mg^{2+} -saturated and glycolated, $CoK\alpha$ radiation; a, b, c, and d show successive details of fit of θ -intervals of the complete pattern. Simulation was carried out with rectorite plus chlorite.

322) were used. The content of K in illite interlayers varied for different samples from 0.62 to 0.89 atoms per $O_{10}(OH)_2$. K, NH_4 , and Na cations were placed in the center of mica interlayers and thicknesses of illite

and tobelite interlayers were 9.98 and 10.33 Å, respectively (Drits *et al.*, 1997a), except for sample DV2 where the thickness of illite interlayers was 10.00 Å. CSD thicknesses were log-normally distributed, the parameters of this distribution were determined using a mean thickness of CSDs and the regression given by Drits *et al.* (1997b). The mean and maximum thicknesses of CSDs were variable parameters.

RESULTS

Rectorite

Rectorite has a well-defined mixed-layer structure with strict periodicity along the c axis and many basal reflections. Rectorite was used to test the profile-fitting procedure since the chemical and structural parameters were well known. In the sample studied, rectorite with chemical composition $(Na_{1.00}K_{0.13}Ca_{0.14}Mg_{0.08})(Al_{4.0})(Si_{6.45}Al_{1.55})O_{20}(OH)_4$ and $d(001) = 26.65$ Å was mixed with a small amount of trioctahedral chlorite, $(Al_{1.80}Mg_{2.45}Fe_{1.50}^{2+})(Si_{2.70}Al_{1.70})O_{10}(OH)_8$ and $d(001) = 14.125$ Å. The rectorite structure was constructed as an ordered alternation of 9.70-Å paragonite layers $(Na_{0.87}K_{0.13}(Si_{3.00}Al_{1.00})Al_{2.00}O_{10}(OH)_2)$ with 16.95-Å glycolated smectite layers, $(Mg_{0.08}Na_{0.13}Ca_{0.13})(Al_2)(Si_{3.45}Al_{0.55})O_{10}(OH)_2 \cdot 6.8(CH_3OH) \cdot 2.6H_2O$. The glycerol-saturated smectite interlayer contains in addition to the exchangeable cations two layers of glycerol molecules whose z coordinates are given by Brindley (1966). Using the z coordinates of Rule and Bailey (1987) for the structure of chlorite with similar chemical composition, the chlorite component was successfully modeled. This modeled pattern was added to the rectorite pattern to obtain a complete fit of the sample diffraction profile.

The experimental and the calculated XRD patterns for the glycolated rectorite are shown in Figure 1. A very good coincidence of positions, intensities, and profiles was achieved for 13 reflection orders of rectorite and seven reflection orders of chlorite. The accuracy of the fitting procedure is demonstrated by the satisfactory agreement between the experimental and calculated patterns for both the glycolated and glycerolated specimens. However, a small disagreement between the experimental and calculated profiles (Figure 1a) is observed for the low-angle part of the 001 rectorite reflection, probably because the influence of the instrumental factors and particularly the Lorenz-polarization effects are not well modeled in this θ region.

Samples B32 and B35

The layer thicknesses, probability parameters, and the fitted XRD curves for the different specimens are shown in Figure 2.

For sample B32, the XRD patterns of the Mg and Na-saturated, air-dried and glycolated specimens and the Ca-saturated and glycolated specimens were suc-

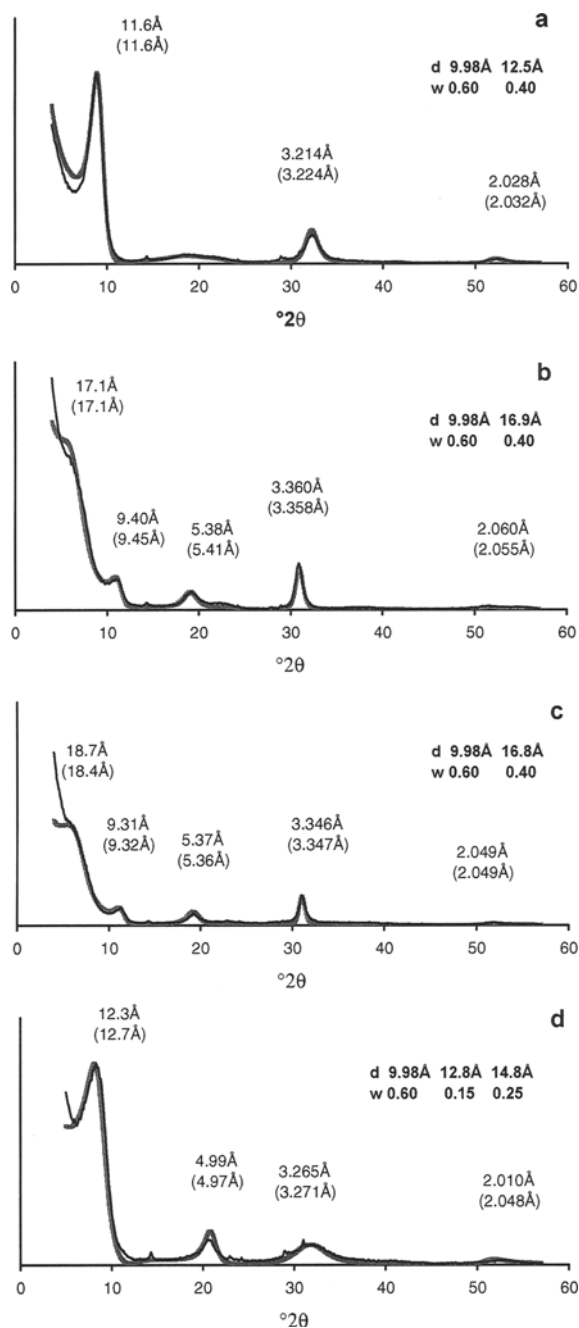


Figure 2. Powder XRD patterns of Kinnekulle Bentonite B32. Observed and simulated patterns shown as solid and shaded lines, respectively; d -values for simulated patterns in brackets; I-S parameters presented above each pattern. Oriented specimens, $\text{CoK}\alpha$ radiation; a) Na^+ -saturated, air-dried, simulated with 2.75 H_2O per $\text{O}_{10}(\text{OH})_2$ (compare Figure 7), b) Na^+ -saturated and glycolated, c) Mg^{2+} -saturated and glycolated, d) Ca^{2+} -saturated and air-dried.

cessfully modeled with a two-component structure having $w_1 = 0.60$ and $R = 0$ (Figure 2a–2c). In contrast, for the Ca-saturated and air-dried specimen, the best fit was obtained for a three-component model. This model has the same number of illite interlayers as the two-component model, and two types of swelling interlayers with thicknesses of 14.8 and 12.8 Å in proportions 0.25 and 0.15, respectively (Figure 2d). In all models, illite interlayers contain 0.85 K per $\text{O}_{10}(\text{OH})_2$.

For sample B35, the same quality of fitting was obtained for Na, Mg, and Ca-saturated specimens with $w_1 = 0.48$ and $R = 0$. As with sample B32, the Ca-saturated and air-dried specimen was fitted with a three-component structural model, but with 48% of 10-Å, 32% of 15.00-Å, and 20% of 13.00-Å layers.

Sample A

Application of I-S models with the usual 9.98 Å thickness of illite layers resulted in a large discrepancy between positions of the calculated and experimental 005 reflections, although the calculated and experimental peak intensities for 001, 002, 003, and 004 coincided for an I-S model with $w_1 = 0.95$ and $R = 0$ (Figure 3a). In contrast, a model having $w_1 = 0.95$, $R = 0$, and a mica-layer thickness of 10.05 Å resulted in satisfactory agreement between peak positions and intensities of all observed basal reflections (Figure 3b). The best fit was obtained for a three-component model in which 9.98-Å illite, 10.32-Å (or 10.35-Å) tobelite or NH_4 -bearing mica, and smectite layers are interstratified with $w_1 = 0.77$, $w_1 = 0.18$, $w_s = 0.05$, and $R = 0$ (Figure 3c). The presence of NH_4 -bearing mica layers was supported by the infrared (IR) spectrum (strong absorption at 1430 cm^{-1}) and by the XRD technique developed by Drits *et al.* (1997c and unpublished data). The smectite interlayers may be distributed with $R \geq 1$ but the XRD pattern is not sensitive to variations in order-disorder relating to the distributions of the small amounts (0.05) of the smectite in this sample.

Sample DV2

For this sample, a one-phase, two-component; a one-phase, three-component; and a two-phase model were tested to obtain the best fit between the experimental and calculated patterns because the experimental patterns deviated from the calculated patterns for the one-phase model at d -values of ~ 4.8 Å.

Two-component model. The probability parameters, layer thicknesses, and the fits of the experimental air-dried and glycolated specimens saturated with the different cations are given in Figure 4. The layer sequence is characterized by near maximum possible degree of order for $R = 2$. Consequently, the layer pairs SS and triplets SSI and ISS are forbidden and the sub-

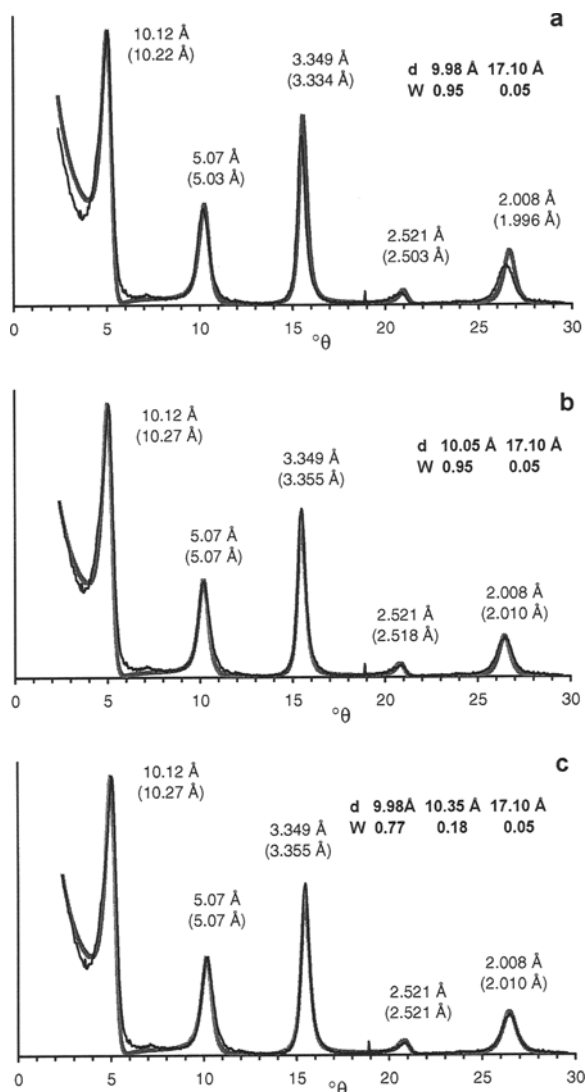


Figure 3. Powder XRD patterns of shale from Karpfsmühle. Observed and simulated patterns shown as solid and shaded lines, respectively; d -values for simulated patterns in brackets; I-S parameters presented above each pattern. Oriented, Mg^{2+} -saturated and glycolated specimen. $CoK\alpha$ radiation. a) Interstratification of 9.98-Å and 17.1-Å layers, b) Interstratification of 10.05-Å and 17.1-Å layers, c) Interstratification of 9.98-Å, 10.35-Å, and 17.1-Å layers.

sequence SIS has a very low probability of occurrence. Illite interlayers have 0.85 of K per $O_{10}(OH)_2$. For the air-dried Na, Mg, and Ca-exchanged specimens, the calculated XRD curves reproduce positions, intensities, and profiles of all basal reflections observed in the experimental XRD patterns (Figure 4a–4c). For the glycolated specimens saturated with Na, Mg, and Ca, the calculated XRD curves show a good fit in position, intensity, and profile of each basal reflection except for those with $d \sim 4.8$ Å. For this peak, the experimental curve is significantly higher than the calculat-

ed, but this difference decreases from Mg to Ca-exchanged specimens (Figure 4d–4f). Changes in composition, structure, proportion, and distribution of glycol-containing smectite interlayers failed to improve the agreement between the observed and the calculated intensities within the 2θ region of 20.6 – 22.8° . For example, an increase in number of glycol molecules increases the intensity of the peak with $d \sim 4.8$ Å, but decreases the intensity of the reflections with $d \sim 5.18$ Å. Similar disagreement for the same diffraction region was observed previously for I-S with $R \geq 1$ (Reynolds, 1980; McCarty and Thompson, 1991). Therefore, more complicated structural models were tested.

Three-component models. It was assumed that the glycolated specimens, in addition to 17-Å smectite layers, contain small amounts of 13-Å vermiculite layers. The amount of illite layers was assumed to be the same as for the two-component model ($w_1 = 0.84$). As little as 0.03 vermiculite layers improved significantly the agreement between calculated and experimental maxima in the region 10 – 11° . However, the presence of vermiculite layers significantly shifts the two reflections in the calculated pattern at small-angle relative to the observed peaks. Therefore, this model was rejected.

A physical mixture of two mixed-layer phases. For glycolated specimens we assume that one interstratified phase produces strong peaks with $d(001) = 9.6$ – 9.7 Å and 5.1 – 5.2 Å, and a second phase shows peaks with $d(001) = 11.8$ – 12.1 and 4.7 – 4.8 Å (Figure 5). A mixture of I-S and I-V phases shows these peaks: the I-S phase consists of 10.00-Å illite and 16.9-Å or 17.0-Å smectite layers with $w_1 = 0.82$, $P_{SS} = 0$, $P_{SIS} = 0.1$, $R = 2$, and the I-V phase of 10.00-Å illite and 13.6-Å vermiculite layers with one layer of glycol molecules and $w_1 = 0.65$ or 0.70 , $P_{VV} = 0$, $R = 1$. Calculated patterns for such I-S and I-V mixed in a ratio of 0.7:0.3 provides better agreement with the maxima of the observed patterns in the region 10 – 11° in comparison with the single two-component model. This model for an I-S and I-V mixture simulates the major diffraction features of the XRD profile for the Mg, Ca, and Na-exchanged, air-dried or glycolated specimens (Figure 5).

Sample 87

Specimens saturated with Mg, Ca, Na, and NH_4 and both air-dried and glycolated were investigated. Layer thicknesses, probability parameters, and the fitted XRD patterns are shown in Figure 6. For all specimens, the structure model has three components, one non-swelling and two swelling. For the Ca, Mg, and Na-saturated specimens, the structure has 10.03-Å illite layers with $w_1 = 0.80$. In Mg or Ca-saturated specimens, both glycolated or air-dried, the two swelling

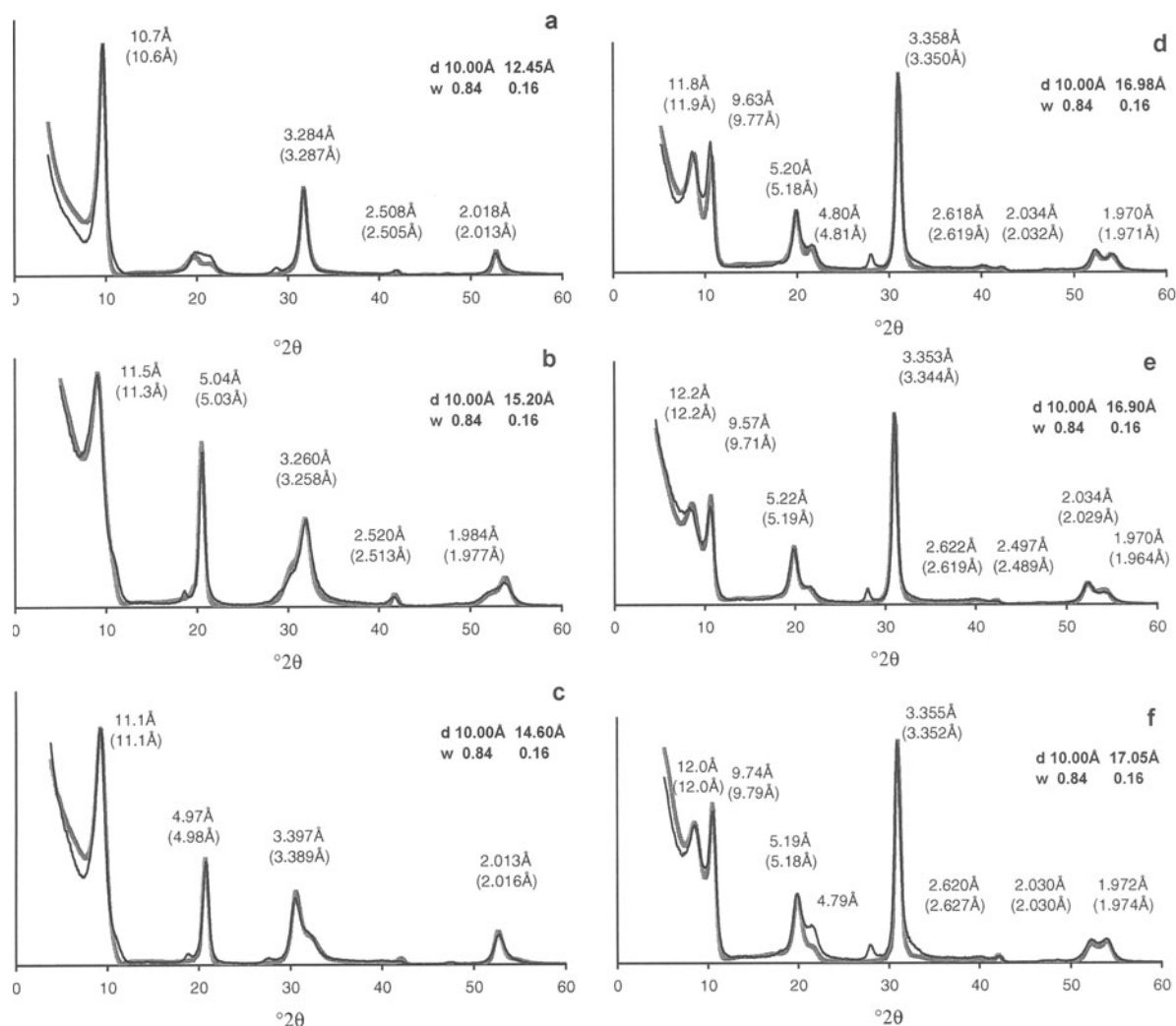


Figure 4. Powder XRD patterns of hydrothermal sample DV2 (Slovakia) simulated as a one-phase I-S. Observed and simulated patterns shown as solid and shaded lines, respectively; d -values of simulated patterns in brackets; I-S parameters are presented above each pattern. Oriented specimens, $\text{CoK}\alpha$ radiation; a) Na^+ -saturated, air-dried, b) Ca^{2+} -saturated and air-dried, c) Mg^{2+} -saturated and air-dried, d) Na^+ -saturated and glycolated, e) Ca^{2+} -saturated and glycolated, f) Mg^{2+} -saturated and glycolated.

components are present in proportions of 0.12 and 0.08 (Figure 6a and 6b) and in the Na-saturated and glycolated specimen in proportions of 0.02 and 0.18 (Figure 6c). The structural models for the Ca, Mg, and Na-saturated, air-dried specimens have 14.0-Å and 12.5-Å expandable layers in proportions of 0.12 and 0.08 (Mg-saturated, Figure 6b), 0.10 and 0.10 (Ca-saturated), Figure 6b), and 0.06 and 0.14 (Na-saturated, Figure 6d), respectively. For the NH_4^+ -saturated, air-dried specimen, the amount of non-swelling layers is 0.90, but 0.10 of these layers have $d(001) = 10.33$ Å. For all models of this sample, the layer types are distributed at $R = 1$.

It is remarkable that the largest part of the swelling component expands to 17.1 Å in the glycolated and Mg and Ca-saturated specimens, but only to 13.35 Å

in the glycolated and Na-saturated specimen. For air-dried specimens, the proportion of layers swelling to 14.0 Å decreases from the Mg-saturated to the Ca-saturated and further to the Na-saturated specimen. The relative humidity in the laboratory was 30–40%.

DISCUSSION

The results show that observed XRD patterns of I-S and I-S-V minerals saturated with different cations and prepared in air-dried and glycolated states can be accurately fitted. However, the multispecimen approach reveals problems in the structural study of these minerals.

Reliability of structural and instrumental parameters

If one set of probability parameters can be used to obtain a satisfactory simulation of experimental XRD

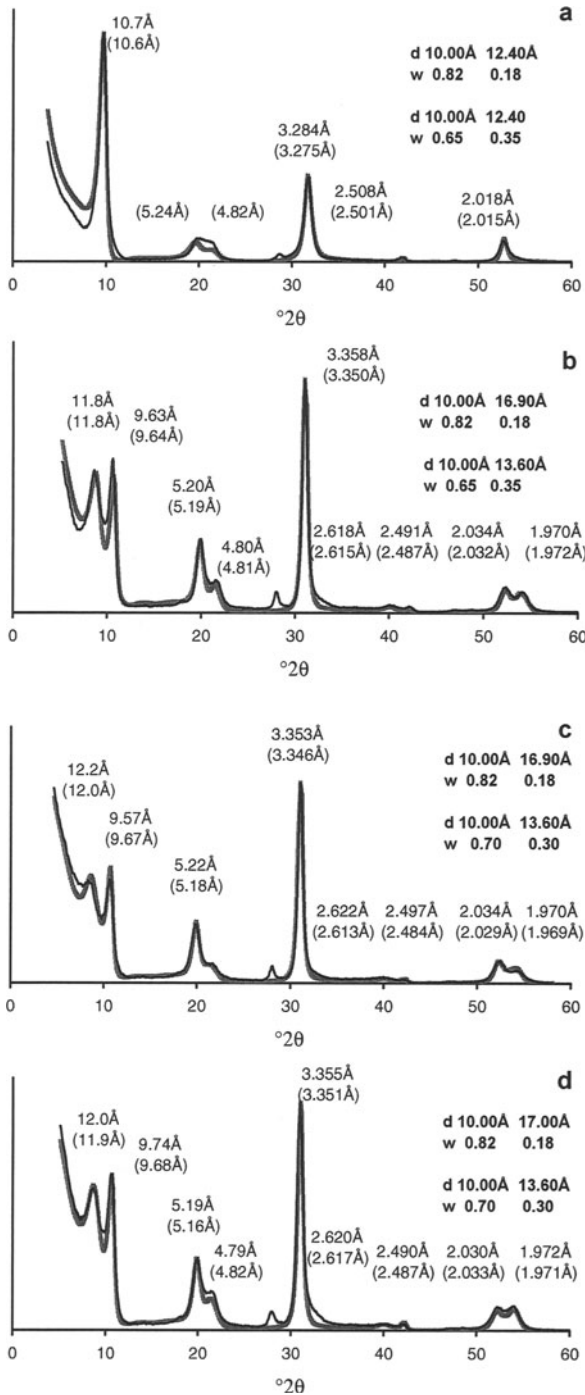


Figure 5. Powder XRD patterns of hydrothermal sample DV2 (Slovakia) simulated as a two-phase mixture of I-S and I-V in the ratio of 2.3:1.0. Observed and simulated patterns shown as solid and shaded lines, respectively; d -values of simulated patterns in brackets; I-S and I-V parameters are presented above each pattern. Oriented specimens, CoK α radiation; a) Na⁺-saturated, air-dried b) Na⁺-saturated and glycolated, c) Ca²⁺-saturated and glycolated, d) Mg²⁺-saturated and glycolated.

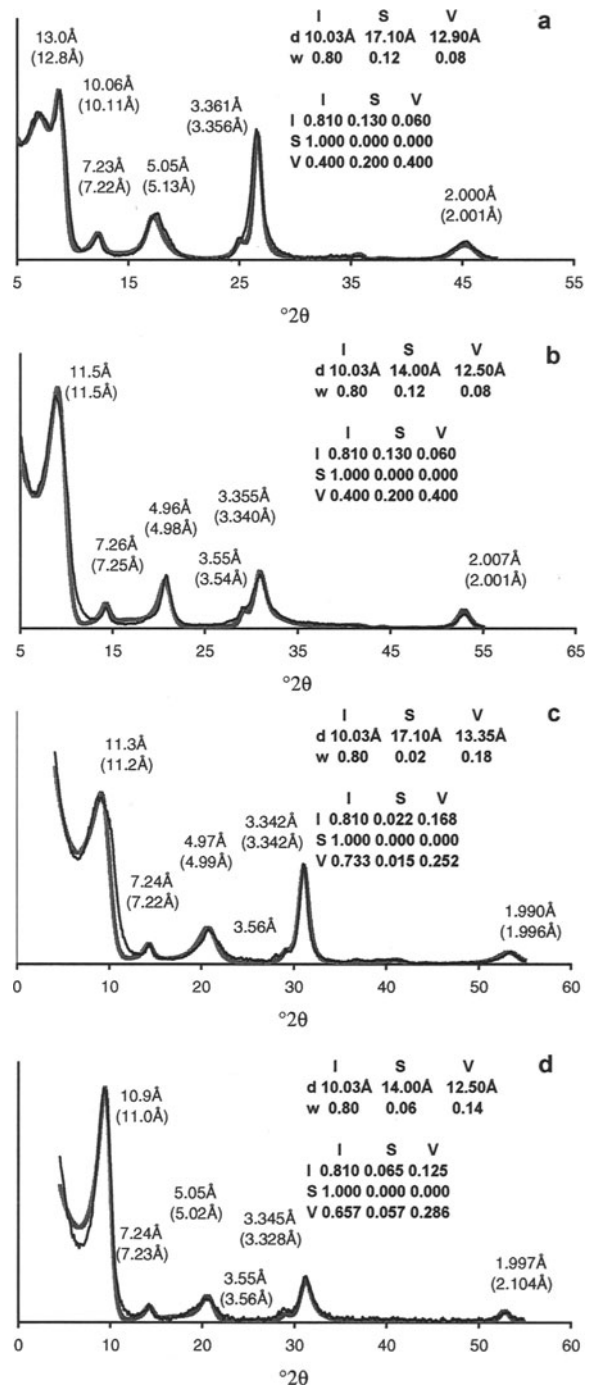


Figure 6. Powder XRD patterns of North Sea Upper Jurassic shale sample from well 2/11-1, 4548 m depth (sample 87). Observed and simulated patterns shown as solid and shaded lines, respectively; d -values of simulated patterns in brackets, I-S-V parameters above each pattern. Oriented specimens, CuK α radiation; a) Mg²⁺-saturated and glycolated, b) Mg²⁺-saturated and air-dried, c) Na⁺-saturated and glycolated, d) Na⁺-saturated, air-dried, CoK α radiation.

Table 1. North Sea well 2/11-1, 4548 m depth (sample 87). Conjective probability parameters for three- and four-component structural models for glycolated specimens.

	Na-saturated								Mg-saturated			
	Three-component			Four-component					Three-component			
	I	S	V	I	S	V'	V	I	S	V		
I	0.810	0.022	0.168	I	0.810	0.022	0.108	0.060	I	0.810	0.130	0.060
S	1.0	0	0	S	1.0	0	0	0	S	1.0	0	0
V	0.733	0.015	0.252	V'	1.0	0	0	0	V	0.4	0.2	0.4
				V	0.400	0.033	0.167	0.400				

patterns for different states (glycolated or air-dried, different exchangeable cations) of one I-S mineral, then the model of layer interstratification must represent the accurate one-dimensional structure along the *c* axis of the mineral. Since the modeled patterns for both the glycolated and glycerolated Na-saturated rectorite showed good agreement to the observed patterns, at least from $2\theta > 3\text{--}4^\circ$ (Figure 1), then the instrumental and sample textural parameters are appropriate. Similarly, the fact that the fits for the different specimens, Kinnekulle B32 and 35, are in good agreement with the observed patterns confirms the validity of the structural model.

For sample 87, only a few of the probability parameters modeled for the different specimens have identical values (Figure 6). The proportion of illite interlayers and the parameters P_{II} , P_{SI} , P_{SS} , and P_{SV} do not change for different specimens, whereas the proportions of the two expandable layer types, w_S and w_V , and P_{IS} , P_{IV} , P_{VI} , P_{VS} , and P_{VV} are different for different specimens. For example, the structural models for the air-dried Mg, Ca, and Na-saturated specimens have 10.03-Å, 14.00-Å, and 12.50-Å layers (Figure 6). However, the proportions of the two last layers for these models are different, 0.12 and 0.08 for the Mg-saturated and 0.06 and 0.14 for the Na-saturated, air-dried specimens, and the values of P_{IS} , P_{IV} , P_{VS} , and P_{VV} are also different. Similar differences between the structural parameters are observed for the glycolated specimens (Figure 6a and 6c). Since the distribution of illite and expandable layers is the same in all specimens after saturation with different cations, the variations must be due to the expandable layers swelling differently depending on the exchangeable cations. For example, for the glycolated specimens saturated with Mg and Na (Figure 6), the amount of two and one-layer glycol interlayers is 0.12 and 0.08 for the Mg-saturated and 0.02 and 0.18 for the Na-saturated specimen. After exchange of Mg by Na, 0.10 of the two-layer glycol interlayers of the Mg-saturated specimen becomes a one-layer glycol complex in the Na-saturated specimen. This complex is similar to the one-layer complex in the vermiculite layers in this specimen. We define layers which in the glycolated state, with each of the exchangeable cations (Ca, Na, Mg), swell to 16.6–17.2 Å and to 12.9–13.6 Å as smectite

and vermiculite layers, respectively. Layers, with swelling properties which depend on the exchangeable cations, are referred to as “low-charge vermiculite or high-charge smectite” layers (V'-layers). In this case, the sample contains 0.02 S, 0.10 V', and 0.08 V layers. For the Mg-saturated specimen, $d(001)_S = d(001)_{V'} = 17.1 \text{ \AA}$, whereas for the Na-saturated specimen $d(001)_V = d(001)_{V'} = 13.35 \text{ \AA}$. The distribution of S, V, and V' layers is identical for all specimens. Accordingly, the parameter sums $w_{IS} + w_{IV}$, $w_{VS} + w_{VV}$, and $w_{SI} + w_{VI}$ for the four-component structure must be equal to w_{IS} , w_{VS} , and w_{SI} , respectively, for the three-component Mg-saturated and glycolated structural model. This is because for this model $V' = S$; and the parameter sums $w_{IV'} + w_{IV}$, $w_{VV'} + w_{VV}$, and $w_{VI} + w_{VI}$ for the four-component model must be equal to w_{IV} , w_{VV} , and w_{VI} , respectively, for the three-component Na-saturated and glycolated structural model. The relationship between the conjuctive probability parameters for the three and four-component systems of the Na- and Mg-saturated glycolated specimens is shown by the matrices in Table 1. From these matrices, the layer pair probabilities $w_{ij} = w_i p_{ij}$ ($i, j = I, S, V, V'$) in the four-component model and the probabilities $w_{ij} = w_i p_{ij}$ ($i, j = I, S, V$) of the three-component models for the Mg and Na-saturated specimens may be calculated to test the above relationships. XRD patterns calculated for the three and four-component systems are identical. Similarly, four-component models were constructed for the Na, Ca, and NH_4 -saturated air-dried specimens. For each specimen, the patterns calculated for the three and four-component mixed-layer models were identical. Thus, the probability parameters of a model with three types of interlayers and a model with four types of interlayers describe accurately the actual mixed-layer structure of each specimen.

For sample DV2, the fitting for all air-dried specimens was satisfactory with one set of values of probability parameters (Figure 4). Thus, the amount, composition, and structure of Ca, Mg, and Na-exchanged smectite interlayers were determined correctly. The poor fit for the reflection at $d \sim 4.8 \text{ \AA}$ for glycolated specimens may be due to the approximate content and mutual disposition of glycol molecules. The problem was partially solved with the two-phase model. Note,

however, that very different models may equally well describe the main diffraction features of the observed patterns for the different treatments. Indeed, the two-component I-S model is very different from the mixture of I-S and I-V. However, apart from the reflection of $d \sim 4.86 \text{ \AA}$, both models produce similar XRD patterns. Thus, for sample DV2, the structure cannot be determined unambiguously by this method.

Accuracy in determination of probability parameters

Reflection intensities are sensitive to small variations of probability parameters and especially to the proportions of interlayers (Drits *et al.*, 1997a). For the Mg-saturated and glycolated sample 87, a change in w_1 from 0.80 to 0.78 or 0.82 results in a marked difference between calculated and observed intensities at least for the first peak (Drits *et al.* 1997a). Thus, if the calculated and observed patterns fit well, then the error in amount of layer types probably is <0.02 . For the air-dried, Na and Mg-saturated specimens of sample DV2 the best fit was obtained with $w_1 = 0.84$, whereas for the Ca-saturated and glycolated specimen the best fit was achieved with $w_1 = 0.82$ (the decrease of 10.00- \AA layers by 0.02 results in a marked improvement in the fit for this specimen). Thus, the proportion of illite interlayers in this sample is equal to 0.84 ± 0.02 . For all air-dried and for the Ca-saturated and glycolated specimen, $P_{\text{SIS}} = 0.10$ whereas the Mg and Na-saturated and glycolated models have $P_{\text{SIS}} = 0.05$ and 0, respectively (Figure 4d–4f). However, the quality of the fit varied for the different glycolated specimens (Figure 4d–4f). Thus, for this sample, the probability parameters for the air-dried specimens were determined with greater reliability and precision than those of the glycolated specimens.

Composition of interlayers

The structure and composition of expandable interlayers in I-S and I-S-V minerals are important for clay-water interaction and thus for swelling properties, and water absorption and desorption of these minerals. According to Środoń *et al.* (1986), illite interlayers in I-S from sandstone, K-bentonites, and hydrothermal deposits contain 0.89 K per $\text{O}_{10}(\text{OH})_2$. Based on this assumption, they proposed a technique for determining mean thickness of illite fundamental particles by using the expandability of I-S minerals.

One advantage of the fitting procedure is the possibility to determine interlayer composition and layer sequences for a mixture of I-S or I-S-V with other minerals. For the hydrothermal sample DV2 and the bentonite samples B32 and B35, the illite interlayers contain 0.85 K per $\text{O}_{10}(\text{OH})_2$ in agreement with Środoń *et al.* (1986). For I-S and I-S-V of North Sea Jurassic and Baltic Cambrian shales, however, the K content in illite interlayers is significantly lower and equal to 0.75 atoms per $\text{O}_{10}(\text{OH})_2$, as for samples 95 and A. More-

over, for the diagenetically transformed shale sample A, the fitting procedure reveals interstratification of K and NH_4 -bearing mica interlayers with the ratio 0.80:0.15. Drits *et al.* (1997c) proposed a technique for determining the amount and distribution of fixed K and NH_4 in I and I-S minerals using the d -values and the full width at half height (FWHH) values of $d(002)$ and $d(005)$ of the K-saturated and heated specimens. For the K-saturated and heated sample A, $d(001) = 5 \times d(005) = 10.031 \text{ \AA}$ and $\text{FWHH}(005)/\text{FWHH}(002) = 1.284$. Accordingly, 15% of 10.33- \AA NH_4 -bearing illite layers are interstratified with 85% of 9.98- \AA K-bearing layers. Based on the fitting, these are 80% of 9.98- \AA illite and 5% dehydrated K-saturated smectite layers. It is remarkable that the proportions of NH_4 in the I-S-V found by the two different approaches are identical. For the diagenetically transformed shale sample 87, simulation shows a composition of 20% expandable interlayers and 0.675 K per $\text{O}_{10}(\text{OH})_2$ in the mica interlayers. Drits *et al.* (1997c) showed that this sample contains 14% of NH_4 -bearing mica interlayers interstratified with K-bearing mica and expandable interlayers. Thus, the ratio of the interstratified K and NH_4 -bearing mica interlayers is equal to 0.825:0.175. Using the scattering power of K and NH_4 as 18 and 10 electrons/ \AA , respectively, the K in the illite interlayers is calculated from the equation: $0.675 = (18 \times 0.825 \times c_K + 10 \times 0.175)/18$. The c_K in illite interlayers is equal to 0.70 K which is similar to the 0.75 for sample 95 and A.

Thus, in conclusion, determination of illite fundamental particle thicknesses based on XRD expandability and the fixed amount of K in illite interlayers needs further refinement for shale I-S and I-S-V minerals. Also, special attention is required for the effective thickness of mica layers in I-S and I-S-V in oil-bearing rocks.

The number of water molecules in smectite interlayers saturated by different exchangeable cations is different for different I-S or I-S-V and the fitting procedure may be used to determine this parameter. Attempts to get a satisfactory fit of sample B32 (Na-saturated, air-dried) with models using the one-dimensional structure for smectite interlayers as proposed by Moore and Reynolds (1989) failed (Figure 7). The best fit was obtained for smectite interlayers containing 2.75 water molecules per $\text{O}_{10}(\text{OH})_2$. Thus, water molecules in smectite interlayers of the I-S structure of sample B32 form a hexagonal planar network where these molecules are separated by $\sim 3.0 \text{ \AA}$. For glycolated interlayers, the fitting procedure applied to the I-S-V of sample 87 confirmed that the amount of glycol molecules in the one-layer glycol interlayer of the vermiculite component is equal to two molecules per $\text{O}_{10}(\text{OH})_2$, the amount given by Moore and Reynolds (1989).

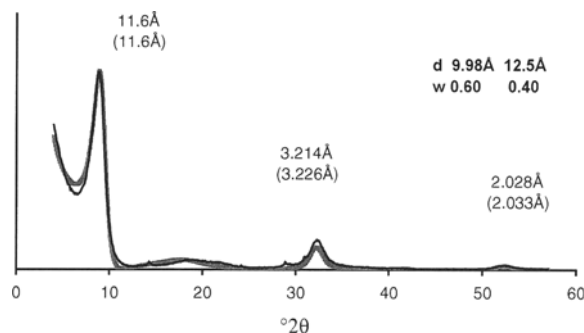


Figure 7. Powder XRD pattern of Kinnekulle Bentonite B32. Observed and simulated patterns shown as solid and shaded lines, respectively; d -values of simulated pattern in brackets, I-S parameters above pattern. Oriented specimen, Na^+ -saturated, air-dried, simulated with 1.0 H_2O per $\text{O}_{10}(\text{OH})_2$ (compare Figure 2a). $\text{CoK}\alpha$ radiation.

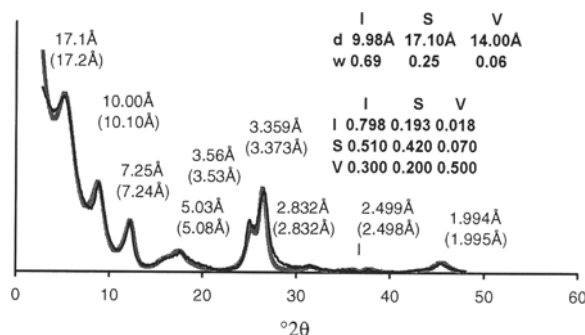


Figure 8. Powder XRD patterns of Danish onshore Upper Jurassic shale sample from well Haldager 1, 1049 m depth (sample 95). Observed and simulated patterns shown as solid and shaded lines, respectively; d -values of simulated patterns in brackets; I-S-V parameters are given in matrix. Oriented specimen, Mg^{2+} -saturated and glycolated. $\text{CuK}\alpha$ radiation.

Segregation of interstratified layer types

Drits and Sakharov (1976) calculated XRD patterns for I-S in which interstratification of illite and smectite layers changed from random alternation to full segregation via intermediate segregated structures. They concluded that XRD patterns for I-S with a significant tendency to segregation are quite similar to XRD patterns from a physical mixture of illite and smectite or illite and I-S. Probably for this reason, at present, it is commonly accepted that alternation of illite and smectite interlayers is random or has some tendency to order but not segregation. From the characteristics of the XRD pattern of Mg -saturated and glycolated sample 95 (Figure 8), the sample may consist of a physical mixture of smectitic, illitic, and kaolinitic phases. Indeed, the diffraction maxima with d -values of 10.0, 5.03, 3.359, and 1.994 Å correspond to an illitic phase containing a small amount of swelling layers, and these layers may explain the small deviation from the d -values of a rational series. If the peak migration curves constructed by Środoń (1984) are applied to the interpretation of these data, then the illitic phase should contain 0% of smectite interlayers. The strong peak with $d = 17.1$ Å might correspond to a smectite phase. An alternative interpretation of the XRD pattern is that sample 95 is a mixture of isolated illite and randomly ordered I-S particles. In this case, the position ($2\theta \sim 15.9^\circ$) of the shoulder from the low-angle side of the reflection with $d = 5.03$ Å (Figure 8) should be considered. Using the technique of Środoń (1980), the content of swelling interlayers in the I-S is equal to 90%, if the 3.359-Å reflection belongs to I-S, and the thickness of the glycolated smectite layers is 16.8 Å.

Attempts to obtain a satisfactory fit for these two-phase models were unsuccessful. However, a satisfactory agreement (Figure 8) between the observed and calculated profiles was achieved for the I-S-V one-

phase models where the layer types have a significant tendency to segregation with the short-range ordering of $R = 1$.

The degree of segregation for each type of layer may be estimated by the expression: $S_i = (P_{ii} - w_i) / (1 - w_i)$, where $i = \text{I, S, or V}$. Accordingly, for $P_{ii} = 1$ then $S = 1$, and the sample contains a phase consisting only of layers of type i . For $P_{ii} = w_i$ and $S_i = 0$, the layers of type i are randomly distributed among the other layer types. For the I-S-V structure of sample 95 the degree of segregation for illite, smectite, and vermiculite layers is: $S_i = 0.35$, $S_s = 0.23$, and $S_v = 0.47$. The values for w_i and P_{ii} ($i = \text{I, S, or V}$) are given in Figure 8. The values of S_i show that the tendency to segregation is different for different layers. These values increase from smectite to vermiculite layers. The significant tendency of vermiculite layers to segregation was found also for the diagenetically transformed North Sea sample 87. As noted from the probability parameters given in Figure 6a and 6b, this I-S-V structure has $S_v = 0.35$. Segregated I-S and I-S-V are probably more common in shales than assumed at present. Distinguishing the mineral mixtures of illite and I-S, or of illite and smectite, from the I-S-V structure having segregated layer types is important for evaluating the parent material and the diagenetic processes.

CONCLUSIONS

The multispecimen method provides one structural model for all samples investigated except for sample DV2, where two different models fitted all observed patterns nearly equally well. Application of the method provides detailed data on the one-dimensional structure for two, three, and four-component systems and on interlayer composition. Thus, interpretation of XRD data from dioctahedral mica-smectite minerals requires analysis of positions as well as of intensities

of all basal reflections in the observed XRD patterns and the interpretation of XRD patterns of glycolated samples may be in error if it is based on the qualitative analysis of a single XRD pattern from a Na-saturated sample.

ACKNOWLEDGMENTS

We are grateful to NATO for the Linkage Grant HTECH.LG and to the Danish Natural Science Research Council for the grant 9601518 without which this investigation would not have been possible. V.A. Drits, B.A. Sakharov, and A. Salyn are grateful to the Russian Science Foundation for financial support.

REFERENCES

- Anderson, J.U. (1963) An improved pretreatment for mineralogical analysis of samples containing organic matter. *Clays and Clay Minerals*, **10**, 380–388.
- Brindley, G.W. (1966) Ethylene glycol and glycerol complexes of smectites and vermiculites. *Clay Minerals*, **6**, 237–259.
- Brusewitz, A.M. (1986) Chemical and physical properties of Palaeozoic bentonites from Kinnekulle, Sweden. *Clays and Clay Minerals*, **34**, 442–454.
- Buzagh, W. and Szepesi, K. (1955) A colloid-chemical method for the determination of the montmorillonite content in bentonites. *Acta Chimica Hungarica*, **5**, 287–298.
- Drits, V.A. and Sakharov, B.A. (1976) *X-ray Analysis of Mixed-layer Minerals*. Nauka, Moscow, 256 pp. (in Russian).
- Drits, V.A. and Tchoubar, C. (1990) *X-ray Diffraction by Disordered Lamellar Structures*. Springer Verlag, Berlin, 371 pp.
- Drits, V.A., Weber, F., Salyn, A.L., and Tsipursky, S.I. (1993) X-ray identification of one-layer illite varieties: Application to the study of illites around uranium deposits, Canada. *Clays and Clay Minerals*, **41**, 389–394.
- Drits, V.A., Varaxina, T.V., Sakharov, B.A., and Plançon, A. (1994) A simple technique for identification of one-dimensional powder X-ray diffraction patterns for mixed-layer illite-smectites and other interstratified minerals. *Clays and Clay Minerals*, **42**, 382–390.
- Drits, V.A., Sakharov, B.A., Lindgreen, H., and Salyn, A. (1997a) Sequential structure transformation of illite-smectite-vermiculite during diagenesis of Upper Jurassic shales from the North Sea and Denmark. *Clay Minerals*, **32**, 351–371.
- Drits, V.A., Šrodoň, J., and Eberi, D.D. (1997b) XRD measurement of mean crystallite thickness of illite and illite/smectite: Reappraisal of the Kubler index and the Scherrer equation. *Clays and Clay Minerals*, **45**, 461–475.
- Drits, V.A., Lindgreen, H., and Salyn, A. (1997c) Determination by X-ray diffraction of content and distribution of fixed ammonium in illite-smectite. Application to North Sea illite-smectites. *American Mineralogist*, **82**, 79–87.
- Gibbs, R.J. (1967) Quantitative X-ray diffraction analysis using clay mineral standards extracted from the samples to be analysed. *Clay Minerals*, **7**, 79–90.
- Hansen, P.L. and Lindgreen, H. (1989) Mixed-layer illite/smectite diagenesis in Upper Jurassic claystones from the North Sea and onshore Denmark. *Clay Minerals*, **24**, 197–213.
- Hower, J., Eslinger, E.V., Hower, M.E., and Perry, E.A. (1976) Mechanism of burial metamorphism of argillaceous sediments. *Geological Society of America Bulletin*, **87**, 725–737.
- Lindgreen, H., Garnaes, J., Besenbacher, F., Laegsgaard, E., and Stensgaard, I. (1992) Illite-smectite from the North Sea investigated by scanning tunneling microscopy. *Clay Minerals*, **27**, 331–342.
- MacEwan, D.M.C. and Wilson, M.J. (1980) Interlayer and intercalation complexes of clay minerals. In *Crystal Structures of Clay Minerals and Their X-ray Identification*, G.W. Brindley and G. Brown, eds., Mineralogical Society, London, 197–248.
- McCarty, D.K. and Thompson, G.R. (1991) Burial diagenesis in two Montana Tertiary basins. *Clays and Clay Minerals*, **39**, 293–305.
- Mehra, O.P. and Jackson, M.L. (1958) Iron oxide removal from soils and clays by a dithionite-citrate buffered with sodium carbonate. *Clays and Clay Minerals*, **7**, 317–327.
- Moore, D.M. and Reynolds, R.C. (1989) *X-ray Diffraction and the Identification and Analysis of Clay Minerals*, Oxford University Press, Oxford.
- Nadeau, P.H. and Reynolds, R.C. (1981) Burial and contact metamorphism in the Mancos shale. *Clays and Clay Minerals*, **29**, 249–259.
- Perry, E. and Hower, J. (1970) Burial diagenesis in Gulf Coast pelitic sediments. *Clays and Clay Minerals*, **18**, 165–177.
- Reynolds, R.C. (1980) Interstratified clay minerals. In *Crystal Structures of Clay Minerals and Their X-ray Identification*, G.W. Brindley and G. Brown, eds., Mineralogical Society, London, 249–304.
- Reynolds, R.C. (1986) The Lorenz-polarization factor and preferred orientation in oriented clay aggregates. *Clays and Clay Minerals*, **34**, 359–367.
- Reynolds, R.C. (1988) Mixed-layer chlorite minerals. In *Hydrous Phyllosilicates (Exclusive of Micas), Reviews in Mineralogy, Volume 19*, S.W. Bailey, ed., Mineralogical Society of America, Chelsea, Michigan, 601–630.
- Reynolds, R.C. and Hower, J. (1970) The nature of interlayering in mixed-layer illite-montmorillonite. *Clays and Clay Minerals*, **18**, 25–36.
- Rule, A.C. and Bailey, S.W. (1987) Refinement of the crystal structure of a monoclinic ferroan clinocllore. *Clays and Clay Minerals*, **35**, 129–138.
- Shutov, V.D., Drits, V.A., and Sakharov, B.A. (1969a) On the mechanism of a postsedimentary transformation of montmorillonite into hydromica. In *Proceedings of the International Clay Conference, Tokyo, 1969, Volume 1*, L. Heller, ed., Jerusalem, 523–532.
- Shutov, V.D., Drits, V.A., and Sakharov, B.A. (1969b) On the mechanism of a postsedimentary transformation of montmorillonite into hydromica: Discussion. In *Proceedings of the International Clay Conference, Tokyo, 1969, Volume 2*, L. Heller, ed., Jerusalem, 126–129.
- Šrodoň, J. (1980) Precise identification of illite/smectite interstratifications by X-ray powder diffraction. *Clays and Clay Minerals*, **28**, 401–411.
- Šrodoň, J. (1981) X-ray identification of randomly interstratified illite/smectite in mixtures with discrete illite. *Clay Minerals*, **16**, 297–304.
- Šrodoň, J. (1984) X-ray powder diffraction identification of illitic materials. *Clays and Clay Minerals*, **32**, 337–349.
- Šrodoň, J., Elsass, F., McHardy, W.J., and Morgan, D.J. (1986) Chemistry of illite/smectite inferred from TEM measurements of fundamental particles. *Clay Minerals*, **27**, 137–158.
- Šucha, V., Kraus, I., Mosser, C., Hroncova, Z., and Siranova, V. (1992) Mixed-layer illite/smectite from the Dovna Ves hydrothermal deposit, the western Carpathians Kremnica MTS, Bratislava. *Geologia Carpathica, Clays, Series 1*, **1**, 13–21.

- Tomita, K., Takahashi, H., and Watanabe, T. (1988) Quantification curves for mica/smectite interstratifications by X-ray powder diffraction. *Clays and Clay Minerals*, **36**, 258–262.
- Watanabe, T. (1981) Identification of interstratifications of illite and montmorillonite by X-ray powder diffraction. *Journal of the Mineralogical Society Japan*, **15**, 32–41. (in Japanese).
- Watanabe, T. (1988) Structural model of illite/smectite interstratified minerals and the diagram for their interstratification. *Clay Science*, **7**, 97–114.
- Weaver, C.E. and Beck, K.C. (1971) Clay water diagenesis during burial: How mud becomes gneiss. *Geological Society of America Special Paper*, **134**, 1–78.
- (Received 1 April 1998; accepted 28 October 1998; Ms. 98-041)